

# Fractional Multi-bit Differential Detection Technique for Continuous Phase Modulation

---

Kee-Hoon Lee and Jong-Soo Seo

**A new low-complexity differential detection technique, fractional multi-bit differential detection (FMDD), is proposed in order to improve the performance of continuous phase modulation (CPM) signals such as Gaussian minimum shift keying (GMSK) and Gaussian frequency shift keying (GFSK). In comparison to conventional one-bit differential detected (1DD) GFSK, the FMDD-employed GFSK provides a signal-to-noise ratio advantage of up to 1.8 dB in an AWGN channel. Thus, the bit-error rate performance of the proposed FMDD is brought close to that of an ideal coherent detection while avoiding the implementation complexity associated with the carrier recovery. In the adjacent channel interference environment, FMDD achieves an even larger SNR advantage compared to 1DD.**

**Keywords:** Differential detection, GFSK.

## I. Introduction

Filtering the data sequence removes the sharp phase transitions of continuous phase modulation (CPM) signals and improves bandwidth efficiency. Murota and Hirade proposed the use of a premodulation Gaussian lowpass filter (GLPF) to shape spectrum of minimum shift keying (MSK) [1]. However, the trade-off of having a more compact spectrum is that the premodulation GLPF introduces inter-symbol interferences in the transmitted signal. Motivated by a performance improvement with a minimum increase in the implementation complexity, we propose a fractional multi-bit differential detection (FMDD) technique which utilizes signals delayed by fractional-bit durations, and demonstrate a bit-error rate (BER) performance improvement of FMDD compared to the conventional one-bit differential detection (1DD). Also note that our proposed FMDD can be used to detect various kinds of CPM signals. For instance, the Bluetooth radio system employs a Gaussian frequency shift keying (GFSK) modulation combined with a 1DD technique because of the good spectral efficiency and low implementation complexity. In this paper, we apply FMDD to GFSK and analyze its BER performance in comparison to that of 1DD-GFSK employed in Bluetooth.

## II. GFSK Transmitter

The output of the FSK modulator can be expressed as

$$p(t) = A_0 \cos[\omega_c t + \phi(t) + \gamma]. \quad (1)$$

In (1),  $A_0$  is a constant envelope of the signal,  $\gamma$  is the initial phase of the carrier (which can be assumed to be zero), and  $\phi(t)$  is the carrier signal phase defined by

---

Manuscript received June 3, 2003; revised Apr. 23, 2004.

This work was supported by the Ministry of Information & Communications, Korea, under the Information Technology Research Center (ITRC) support program.

Kee-Hoon Lee (phone:+82 2 2123 2878, email: powerlee@yonsei.ac.kr) and Jong-Soo Seo (email: jsseo@yonsei.ac.kr) are with the Department of Electrical and Electronic Engineering, Yonsei University, Seoul, Korea.

$$\phi(t) = 2\pi h \int_{-\infty}^t y(\tau) d\tau = k_m \sum_{i=-\infty}^{\infty} 2\pi h \int_{-\infty}^t g(\tau - iT) d\tau, \quad (2)$$

where  $g(t)$  is an impulse response of the transmit LPF (i.e., GLPF for GFSK) to a unit amplitude rectangular pulse of duration  $T$ .

A transmitted GFSK signal also can be represented [2] as

$$p(t) = \text{Re} \left\{ \sqrt{\frac{2E}{T}} \exp \left[ j2\pi \left( f_c t + h \int_{-\infty}^t y(\tau) d\tau \right) \right] \right\}, \quad (3)$$

where  $E$  is the energy per symbol,  $T$  is the data bit-duration,  $f_c$  is the carrier frequency,  $h$  is the modulation index, and  $y(t)$  is the output of a GLPF. The values of  $h$  and  $BT$  (3 dB bandwidth,  $B$  of GLPF, and  $T$  product) employed for GFSK are 0.28 to 0.35 and 0.5, respectively. A typical block diagram of a GFSK transmitter, corresponding to (3), is shown in Fig. 1(a).

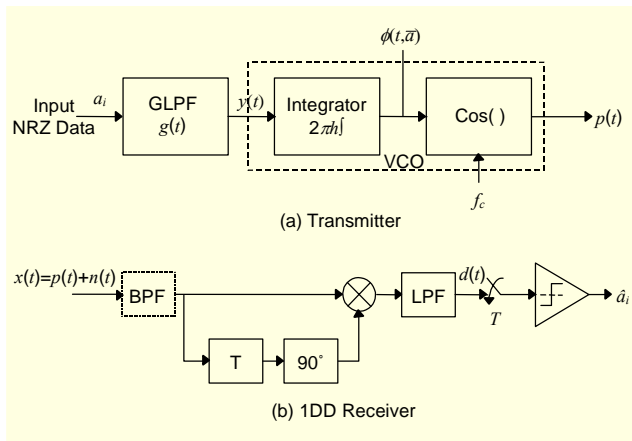


Fig. 1. Block diagram of a GFSK transmitter and 1DD receiver.

### III. 1DD Receiver

The block diagram of a conventional 1DD is illustrated in Fig. 1(b). The signal at the input of the predetection bandpass filter is corrupted by additive white Gaussian noise  $n(t)$  with a one-sided spectral density  $N_0$ . The received signal  $x(t)$  and the signal at the output of the predetection bandpass filter  $x'(t)$  can be represented as

$$x(t) = p(t) + n(t), \quad (4)$$

$$x'(t) = A(t) \cos[\omega_c t + \phi'(t)] + n_{bp}(t), \quad (5)$$

where  $A(t)$  is the time-varying envelope of the signal,  $\omega_c = 2\pi f_c$  is the carrier frequency,  $\phi'(t)$  is the distorted signal phase, and  $n_{bp}(t)$  is the narrow-band Gaussian noise. For

a mathematical analysis in the ideal AWGN channel which follows, we shall assume that  $\phi'(t) = \phi(t)$  and  $A(t) = 1$ . However, for a more practical simulation of the system performance, the time-varying channel distortion due to the filtering is considered. When the received signal is multiplied by the 1-bit delayed received signal, the obtained baseband signal in the absence of noise is

$$d(t) = \sin[\phi(t) - \phi(t - T)]. \quad (6)$$

### IV. FMDD Receiver

A block diagram of FMDD is illustrated in Fig. 2. Assuming that the over-sampling rate of the received signal is  $f_s (= 1/T_s = m/T)$  and the number of delayed samples is  $\delta$ , the delay of the fractional-bit differential detector (FDD) can be expressed as  $(\delta/m)T$ . Hereafter, we will use  $k (= \delta/m)$  as a notation of the unit fractional number.

From (7) to (10), to simplify the mathematical analysis, we shall consider only the noiseless signal. The received signal multiplied by its complex conjugate that is delayed by a multiple of the unit fractional-bit duration is represented as

$$x(t - \lambda kT)_{90^\circ} = A(t - \lambda kT) \cos[\omega_c(t - \lambda kT) + \phi(t - \lambda kT) + 90^\circ], \quad (7)$$

where  $\lambda$  is an integer and denotes the branch number of the FDD. The output of the FDD after removing the second harmonic terms is

$$\begin{aligned} r_{\lambda k}(t) &= x(t)x(t - \lambda kT)_{90^\circ} \\ &= \frac{A(t)A(t - \lambda kT)}{2} \sin[\omega_c \lambda kT + \Delta\phi(\lambda kT)], \end{aligned} \quad (8)$$

where  $\omega_c \lambda kT$  is a phase offset contributed by the FDD (whereas the output of 1DD contains no phase-offset term), and  $\Delta\phi(\lambda kT)$  is

$$\Delta\phi(\lambda kT) = \phi(t) - \phi(t - \lambda kT), \quad (9)$$

which represents the change of signal phase over a fractional-bit duration.

The threshold detector of the FDD decides that a “1” was sent if  $r_{\lambda k}(t) > 0$  and a “0” otherwise. Since envelope  $A(t)$  is always positive, the equivalent decision rule is, decide that a “1” was sent if  $\sin[\omega_c \lambda kT + \Delta\phi(\lambda kT)] > 0$  and a “0” if  $\sin[\omega_c \lambda kT + \Delta\phi(\lambda kT)] < 0$ .

Let's first consider the phase offset  $\omega_c \lambda kT$  in (8). Assuming

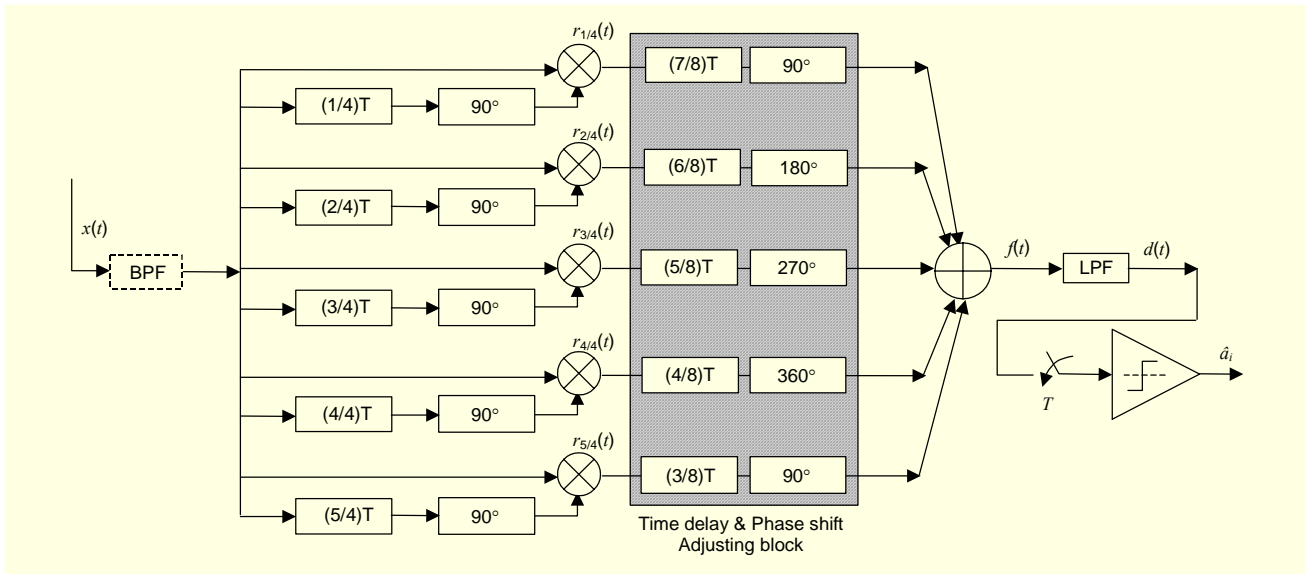


Fig. 2. Block diagram of a GFSK receiver employing a five-fold FMDD.

$f_c = nf_B = n/T$  for an integer  $n$ , we can replace  $\omega_c \lambda k T$  by  $2\pi n \lambda k (= 2\pi n/T \cdot \lambda k T)$ . If we choose the values  $n$  and  $k$  to satisfy  $nk = l$  for integer  $l$ , the one-bit decision rule is still applicable to the FDD regardless of  $\omega_c \lambda k T$ . However, for  $nk \neq l$ ,  $\omega_c \lambda k T$  should be compensated by adding complementary phase shift  $\psi_{\lambda k}$  (i.e.,  $\omega_c \lambda k T + \psi_{\lambda k} = 2\pi$ ) prior to combining all the outputs of the FDD branches of FMDD. In Table 1, the values of  $\omega_c \lambda k T$  are tabulated for various combinations of  $\lambda$  and  $nk$  for  $k=1/4$ . Second, we need to consider the timing delay offset contributed by fractional-bit delay  $\lambda k T$  of every FDD branch. This offset is also required to be compensated by adding complementary time delay  $D_{\lambda k} T$  (i.e.,  $\lambda k T + D_{\lambda k} T = \text{constant time delay}$ ). Note that  $n, k, \lambda, \psi_{\lambda k}$  and  $D_{\lambda k} T$  are the design parameters to be implemented in the FMDD receiver. Table 2 lists the complementary phase shift and time delay required for various fractional-bit delays of the FDD branches of a five-fold FMDD.

In the case of a GFSK receiver employing a five-fold FMDD, by combining a 1-bit differential detected signal and four additional fractional-bit differential detected signals, a five-fold FMDD can improve BER performance. It should be noted that the number of available branches for FMDD depends on  $k$ , the response of the transmit filter, and bit duration  $T$ . The smaller the value of  $k$ , and/or the larger the transmit filter  $BT$  product, the larger the number of available branches. The number of FMDD branches can be optimized corresponding to a trade-off between its performance and hardware complexity.

Table 3 compares the implementation complexity of various receiver schemes [3], [4] including FMDD. The implementation

Table 1. Phase-offset for various combinations of  $\lambda$  and  $n(=f_c/f_B)$ , when  $k=1/4$ .

$\lambda$	Phase-offset ( $\omega_c \lambda k T = 2\pi n \lambda k$ ) for $k=1/4$				
	$n=1$	$n=2$	$n=3$	$n=4$	$n=\alpha$ (integer)
1	$(1/2)\pi$	$\pi$	$(3/2)\pi$	$2\pi$	$(1/2)\alpha\pi$
2	$\pi$	$2\pi$	$\pi$	$2\pi$	$\alpha\pi$
3	$(3/2)\pi$	$\pi$	$(1/2)\pi$	$2\pi$	$(3/2)\alpha\pi$
4	$2\pi$	$2\pi$	$2\pi$	$2\pi$	$2\pi$
5	$(1/2)\pi$	$\pi$	$(3/2)\pi$	$2\pi$	$(1/2)\alpha\pi$
6	$\pi$	$2\pi$	$\pi$	$2\pi$	$\alpha\pi$
7	$(3/2)\pi$	$\pi$	$(1/2)\pi$	$2\pi$	$(3/2)\alpha\pi$
8	$2\pi$	$2\pi$	$2\pi$	$2\pi$	$2\pi$

Table 2. Complementary phase shift and delay time corresponding to various timing delays of FDD branches of five-fold FMDD, when  $k=1/4$ .

Bit delay ( $\lambda k T$ )	Time delay ( $D_{\lambda k} T$ )	Phase shift ( $\psi_{\lambda k}$ )
$kT$	$(7/8)T$	$90^\circ$
$2kT$	$(6/8)T$	$180^\circ$
$3kT$	$(5/8)T$	$270^\circ$
$4kT$	$(4/8)T$	$360^\circ$
$5kT$	$(3/8)T$	$90^\circ$

**Table 3.** Implementation complexities of an FMDD receiver and other receiver schemes.

Receiver scheme	Composing elements				
	DD	<u>MLSE</u>	DF or VA	<u>LPF</u>	Delay & phase adjustment
1DD (or 2DD, 3DD)	1	None	None	1	None
1+2DF <sup>1)</sup>	2	None	1 (DF)	2	2
2+3DF <sup>2)</sup>	2	None	1 (DF)	2	4
$\Lambda$ -bit Differential MLSE	$\Lambda$	1	None	$\Lambda$	$\Lambda$
Coherent <sup>3)</sup> MLSE with Viterbi- algorithm	None	1	1 (VA)	1	None
$\Lambda$ - fold FMDD	$\Lambda$	None	None	1	$\Lambda$

notes: 1) 1+2DF scheme employs a decision feedback (DF) logic. [4]  
 2) 2+3DF scheme employs two DF logics, as well as a differential encoder.  
 3) Coherent receiver needs an additional carrier recovery.

complexity of the maximum likelihood sequential estimation (MLSE) receiver using the Viterbi algorithm increases exponentially with the number of detector memory [3]. In Table 3, the bold and underlined components are the ones which dominantly affect the implementation complexity of the receiver. We found that, except for 1DD (or 2DD and 3DD), FMDD can be implemented with the lowest complexity.

The FMDD output signal  $f(t)$  can be expressed as

$$f(t) = \sum_{\lambda=1}^{\Lambda} r_{\lambda k} t - D_{\lambda k} T_{\psi_{\lambda k}}, \quad (10)$$

where  $\lambda(1 \leq \lambda \leq \Lambda)$  denotes the number of branches, of which the total number is  $\Lambda$ , and  $D_{\lambda k} T$  and  $\psi_{\lambda k}$  denote the timing delay offset and phase offset to be adjusted prior to combining the outputs of all FDD branches. From (7) to (10) the resultant phase state of  $\Lambda$ -fold FMDD,  $\Delta\Phi_{FMDD}$  can be defined as,

$$\exp^{-j\Delta\Phi_{FMDD}} = \frac{1}{\Lambda} \sum_{\lambda=1}^{\Lambda} \exp^{-j\Delta\Phi_{\lambda k}}, \quad (11)$$

$$\begin{aligned} \Delta\Phi_{\lambda k} &= \phi_i - \phi_{i-\lambda k} + \eta_i - \eta_{i-\lambda k} \\ &= \Delta\phi_{\lambda k} + \Delta\eta_{\lambda k} \end{aligned}, \quad (12)$$

where  $\Delta\phi_{\lambda k}$  and  $\Delta\eta_{\lambda k}$  respectively denote the variations of the signal phase and phase shift introduced by AWGN and detected by the  $\lambda k$ -FDD branch over a fractional ( $\lambda k$ )-bit period.

Since the decision rule  $\hat{a}_i = \text{sgn}[f(t)]$  is independent of

envelope variations, if the detected phase of every FDD branch is small enough, (11) can be rewritten as

$$\begin{aligned} \Delta\Phi_{FMDD} &= \frac{1}{\Lambda} \sum_{\lambda=1}^{\Lambda} \Delta\Phi_{\lambda k} \\ &= \frac{1}{\Lambda} \sum_{\lambda=1}^{\Lambda} \Delta\phi_{\lambda k} + \eta_{FMDD} \end{aligned}, \quad (13)$$

where

$$\eta_{FMDD} = \frac{1}{\Lambda} \sum_{\lambda=1}^{\Lambda} \Delta\eta_{\lambda k}. \quad (14)$$

Since  $\Delta\eta_{\lambda k}$  can be assumed to be uniformly distributed in  $(-\pi, \pi)$ , the phase shift can be minimized by FMDD, and an improved BER performance can be achieved.

In the ACI environments, the input signal  $r(t)$  to the receiver includes the transmitted signal  $x(t)$ , ACI signals, and the AWGN  $n(t)$ , i.e.,

$$r(t) = x(t) + i^+(t) + i^-(t) + n(t), \quad (15)$$

where  $i^+(t)$  and  $i^-(t)$  denote the signals of the upper and lower ACIs which contribute most significantly to the degradation of telecommunication systems. We assume that both of them are symmetrically located in the frequency domain around  $f_c$  separated by the channel spacing  $\Delta F$ . In the simulation, we assume that the interfering signals have the same power as the desired signal.

The resultant phase state of 1DD, taking into account both the interfering ACI channels and the AWGN, is defined as  $\Delta\Phi'_{1DD}$  and expressed as

$$\Delta\Phi'_{1DD} = \Delta\phi' + \Delta\eta + \Delta\zeta^+ + \Delta\zeta^-, \quad (16)$$

where  $\Delta\zeta^+$  and  $\Delta\zeta^-$  denote the variations of the arbitrary phase shift introduced by the signals of the upper and lower interferers,  $i^+(t)$  and  $i^-(t)$ , respectively.

The resultant phase state of  $\Lambda$ -fold FMDD, taking into account both the interfering ACI channels and the AWGN, is defined as  $\Delta\Phi'_{FMDD}$  and expressed as

$$\begin{aligned} \Delta\Phi'_{\lambda k} &= \frac{1}{\Lambda} \sum_{\lambda=1}^{\Lambda} \Delta\Phi'_{\lambda k} \\ &= \frac{1}{\Lambda} \sum_{\lambda=1}^{\Lambda} (\Delta\phi'_{\lambda k} + \Delta\eta_{\lambda k} + \Delta\zeta'_{\lambda k}), \quad (17) \\ &= \frac{1}{\Lambda} \sum_{\lambda=1}^{\Lambda} \Delta\phi'_{\lambda k} + \eta_{FMDD} + \zeta_{FMDD} \end{aligned}$$

where  $\Delta\zeta'_{\lambda k}$  is the variation of arbitrary phase shift introduced by the two adjacent channels, which can be assumed to have a

uniform distribution in a  $(-\pi, \pi)$  range. We heuristically found in (16) and (17) that FMDD can effectively minimize the effects of noise and ACI, whereas, 1DD is very sensitive to them.

### V. Analysis of BER Performance

Based on the above discussion, the average probability of bit error  $P_b$  of FMDD-GMSK can be expressed as

$$P_b = \frac{1}{2} \overline{\Pr\{\sin \Delta\Phi_{FMDD}(T) < 0 \mid d(t), "1" \text{ sent}\}} + \frac{1}{2} \overline{\Pr\{\sin \Delta\Phi_{FMDD}(T) > 0 \mid d(t), "0" \text{ sent}\}} \quad (18)$$

where  $d(t)$  and the overbar denote the receive lowpass filtered version of  $f(t)$  and the statistical averaging over all equally likely input data sequences, respectively. Note that when  $\Lambda=1$  and  $k=1$ ,  $P_b$  of FMDD is the very  $P_b$  of 1DD.

### VI. Simulation Results

The performance of FMDD-GFSK is simulated using the SPW (Signal Processing Worksystem). The demodulated signal is passed through a GLPF, of which the optimum 3 dB bandwidth was found to be 1.1 times the Nyquist frequency. Figure 3 illustrates that FMDD outperforms 1DD and the corresponding SNR advantage is increased in proportion to the number of FDD branches. We noticed that five-fold FMDD-GFSK outperforms 1DD-GFSK by 1.8 dB at  $BER=1 \times 10^{-4}$  in an AWGN channel. Figure 4 compares the BER performances of three- and five-fold FMDD receivers with those of various MLSE receivers [3]. We found that three-fold and five-fold FMDD outperform all the other MLSE differential detectors.

The received GFSK signal corrupted by ACI (channel

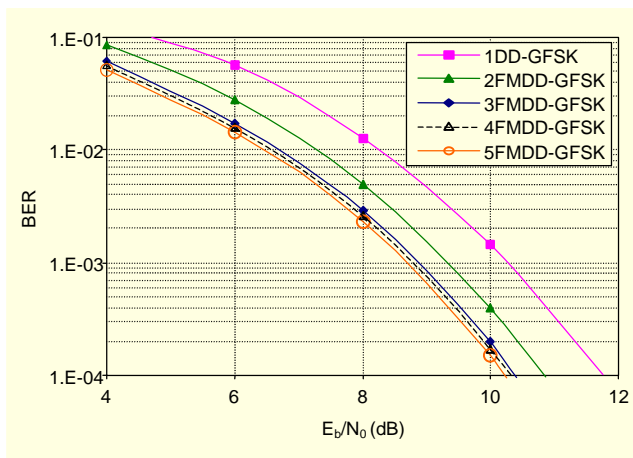


Fig. 3. BER performance of 1DD-GFSK and FMDD-GFSK in an AWGN channel ( $\Lambda$ FMDD :  $\Lambda$ -fold FMDD).

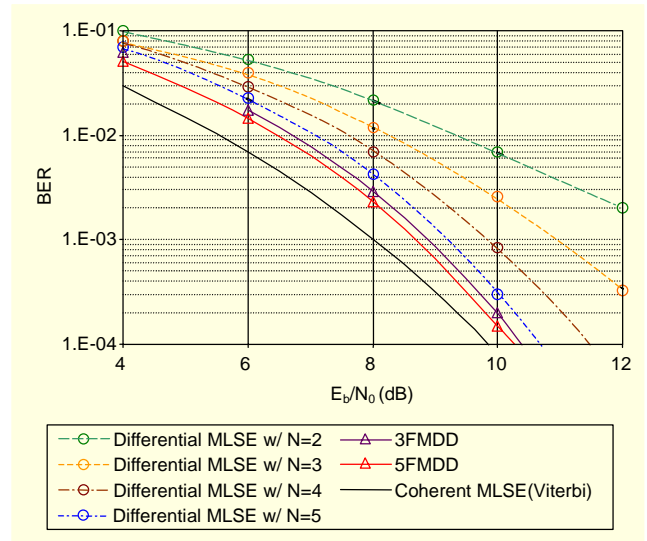


Fig. 4. BER performance of FMDD receivers and MLSE receivers ( $N$  : length of sequence).

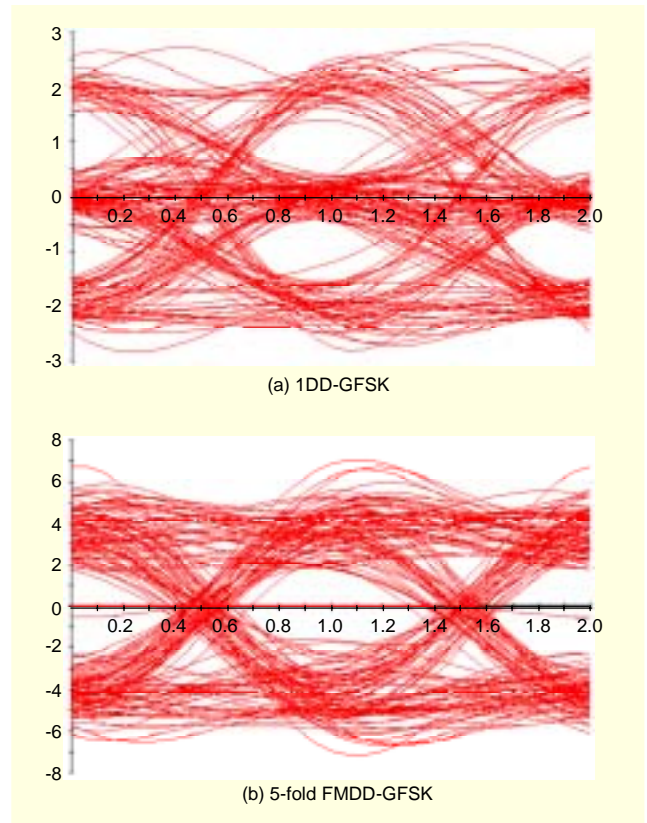


Fig. 5. Demodulated eye-diagrams of GFSK in an ACI environment ( $\Delta F = 1.5 \times f_B$ ,  $E_b/N_o = 20$  dB).

spacing  $\Delta F = 1.5 \times$  data bit rate,  $E_b/N_o = 20$  dB) is simulated, and the corresponding eye diagrams of 1DD-GFSK and five-fold FMDD-GFSK are shown in Figs. 5(a) and 5(b), respectively. From Fig. 5, we clearly observed that an FMDD

receiver is much more robust than a 1DD receiver. The BER performance of five-fold FMDD-GFSK as well as 1DD-GFSK in the presence of AWGN and ACI is also evaluated for various channel spacing. Figure 6 demonstrates that five-fold FMDD-GFSK significantly outperforms a 1DD-GFSK receiver in various ACI environments.

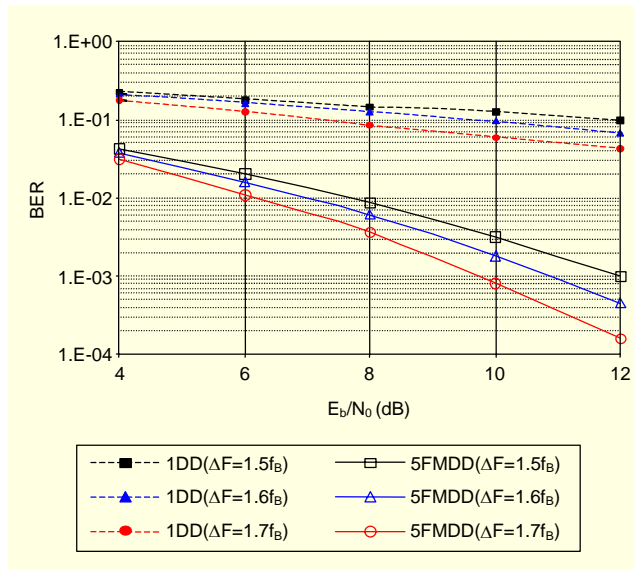


Fig. 6. BER performance of 1DD-GFSK and five-fold FMDD-GFSK in AWGN and ACI environments.

## VII. Conclusion

A new low-complexity FMDD technique is proposed in order to improve the BER performance of differentially detected CPM signals such as GMSK and GFSK. Our simulation results show that five-fold FMDD-GFSK provides an SNR advantage of up to 1.8 dB at  $BER=1 \times 10^{-4}$  in an AWGN channel, and achieves an even larger improvement in spectrally congested ACI environments.

## References

- [1] K. Murota and K. Hirade, "GMSK Modulation for Digital Mobile Radio Telephony," *IEEE Trans. on Commun.*, vol. COM -29, July 1981, pp. 1044-1050.
- [2] C.-H. Park et al., "Channel Estimation and DC-Offset Compensation Schemes for Frequency-Hopped Bluetooth Networks," *IEEE Commun. Lett.*, vol. 5, no. 1, Jan. 2001, pp. 4-6.
- [3] A. Abrardo, G. Benelli, and G.R. Cau, "Multiple-Symbol Differential Detection of GMSK for Mobile Comm.," *IEEE Trans. on Veh. Technol.*, vol. 44, Issue: 3, Aug. 1995, pp. 379 - 389.

- [4] A. Yongacoglu, D. Makrakis, and K. Feher, "Differential Detection of GMSK Using Decision Feedback," *IEEE Trans. on Commun.*, vol. 36-6, June 1988, pp. 641 - 649.



**Kee-Hoon Lee** was born in Boseong, Korea, in 1965. He received the BS degree in aeronautical engineering from the ROK Air Force (ROKAF) Academy, Cheong-ju, Korea, in 1987, the MS degree from University of Dayton, Ohio, USA, in 1996, and the PhD degree in electrical and electronics engineering from Yonsei University,

Seoul, Korea, in 2004. Since joining the ROKAF in 1987, he has been working as an Information and Communications Officer. His current research interests are in the areas of digital modems, satellite communication systems, and standard time & frequency dissemination systems.



**Jong-Soo Seo** received the BS degree in electrical engineering from Yonsei University, Seoul, Korea, in 1975 and the MS and PhD degrees from the University of Ottawa, Canada in 1983 and 1988, respectively. He worked in IDC and CAL, Canada, for digital satellite and broadcasting systems for six years. Since 1995,

he has been with the Department of Electrical and Electronics Engineering at Yonsei University, Seoul, Korea, where he is a professor. He has three international patents in relative areas and has published about 20 IEEE papers. Since Nov. of 2001, he has been a director of the Direct Center for Advanced Broadcasting Technology. His current research interests include digital modems and digital broadcasting.